

Solar Radiation Measurements from Greenland to Antarctica - Optics Table Data from the Danish Galathea III Expedition 2006-2007

Frank Bason, SolData Instruments
soldata@soldata.dk, Silkeborg, Denmark

ABSTRACT

The Danish Galathea 3 Expedition recently completed an eight month journey of exploration and discovery, setting sail from Copenhagen on August 11th, 2006, and returning there on April 25th, 2007. SolData Instruments was privileged to be selected to contribute an “optics table” with pyranometers, ultraviolet, lux, sky luminance, PAR and other optical radiation detectors. These instruments recorded data continuously during the 100.000 kilometer voyage of the Royal Danish Navy vessel *Vædderen*. The voyage provided global solar irradiance and other data as far north as the Arctic Circle near Greenland and as far south as Antarctica. The data collected was analyzed to validate a solar irradiance model described in this paper. A unique opportunity was also provided to check the performance of inexpensive SolData photovoltaic pyranometers against data from a Kipp-Zonen CM11 instrument. In addition to optical radiation, ionizing radiation and atmospheric pressure were also measured, and some interesting aspects of these measurements will also be mentioned.

THE EQUIPMENT

The data logger used was a CR10X from Cambridge Scientific which provided half a dozen analog input channels and a number of digital inputs. The data logger, power supplies etc. were mounted inside the hydrographics laboratory container and connected to a PC with data logger control software. A ca. 20 meter long cable connected the data logger to the instruments on the optics table mounted on top of the container.



Figure 1: *The The Royal Danish Navy vessel Vædderen served as instrument platform for the SolData optics table during the 100.000 kilometer, eight month round the world voyage of exploration and scientific research. It was conducted under the auspices of the Danish Galathea 3 Expedition. Previous Galathea expeditions sailed from Denmark in 1845 and 1950.*



Figure 2: *The optics table was an aluminum frame firmly fastened to the aft port side of the vessel near the rail. The sky luminance sensor (at right) points towards the horizon with an elevation angle of about 10 degrees. The two SolData photovoltaic pyranometers are visible at the left rear behind the Kipp-Zonen CM 11. In the foreground are a UVB detector and a lux detector. The Geiger-Müller detector at the right measured ionizing radiation.*

Table I provides an overview of the instrumentation on the optics table. The three pyranometers were used for mutual control and calibration. Other light detectors measured illuminance (lux) and sky luminance (candela per square meter) and UVB (ultraviolet intensity units UVI). A PAR (photosynthetically active radiation) detector was also connected to our data logger. An atmospheric pressure sensor inside the laboratory and the ionizing radiation detector were also in use.

DATA COLLECTION

Our data was recorded in the same fashion as is standard practice for the Danish Met Office: 10 minute averages are recorded every 10 minutes. In the case of the GM counter the total number of counts during each 10 minute interval was recorded. All data records were date and time stamped with the UTC time. An e-mail was sent by a technician on board weekly with data from Monday through Sunday. The raw data were then transferred in a block to an Excel spreadsheet for calibration, unit conversions, graphics and other data analysis. This database was updated weekly throughout the duration of the voyage. It is currently available to all at the internet address:

www.soldata.dk

There were an average of 20-30 research scientists and graduate students continuously engaged in their own projects, and many additional data (acidity, salinity, sea surface temperature, CO₂ content, dissolved oxygen, etc.) were collected throughout the voyage. The expedition database is accessible via the Galathea 3 Expedition home page.

Instrument	Measures (units)	Sponsor
Kipp-Zonen CM11 pyranometer	Global irradiance on horizontal surface (W/m ²)	SolData Instruments, Silkeborg, Denmark
SolData 80spc, 2 ea.	Global irradiance on horizontal surface (W/m ²)	SolData Instruments, Silkeborg, Denmark
UVB detector	Ultraviolet B-band radiation (UVI)	Frederiksen A/S, Ølgod, Denmark
LUX detector	Illuminance on horizontal surface (lux lumen/m ²)	Frederiksen A/S, Ølgod, Denmark
GM counter	Background radiation summed over 10 minute intervals.	Frederiksen A/S, Ølgod, Denmark
Barometer (inside laboratory)	Atmospheric pressure in hectopascal (hPa)	SolData Instruments, Silkeborg, Denmark
Sky luminance detector	Sky luminance (candela/m ²)	SolData Instruments, Silkeborg, Denmark
PAR detector	Photosynthetically Active Radiation (einstein/m ²)	National Environmental Research Institute (NERI)

Table I: Brief description of the SolData optics table instrumentation on board the research vessel *Vædderen* during the Galathea 3 Expedition.

SOLAR GLOBAL IRRADIANCE

Clear weather predominated during the Galathea Expedition. Many days were “perfect” clear

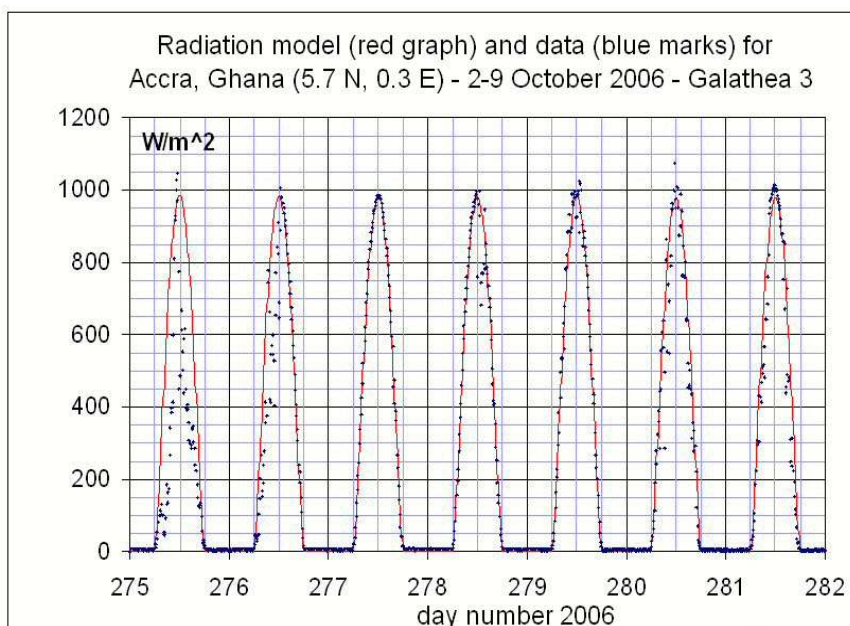


Figure 3: The Galathea Expedition provided a unique opportunity to measure global solar irradiance over a wide range of locations, solar elevation angles and temperatures. The data shown was measured using a Sol-Data 80spc pyranometer. It was continuously checked against a second 80spc and with a Kipp-Zonen CM-11 pyranometer. Sunny days were by far the predominant weather type during the 8 month 100.000 kilometer voyage.

days as can be seen in Figure 3 which shows data from the harbor of Accra, Ghana, collected in October 2006. Data from the optics table have yielded the clear day global irradiance on a horizontal surface for a wide range of geographic locations and atmospheric conditions.

Fine, clear days are ideal for testing radiation models which aim to predict the global solar irradiance on the horizontal as a function of the time of day, location on the earth's surface and the solar declination angle. This knowledge is valuable in connection with the design of solar energy systems, photovoltaic and thermal, as well as for use in agriculture and in computations of the energy balance of the earth in climate modelling. Consider now the following equation describing the *global irradiance*, i.e. the sum of the direct solar irradiance striking the surface and the diffuse irradiance from the sky and from clouds.

$$I_G = I_0 F_J a^L \sin V + I_F \quad (1)$$

The first term takes the *direct irradiance* into account, and the second corresponds to the *diffuse irradiance* from the sky and from clouds. Note that the direct irradiance term contains the *solar constant* $I_0 = 1367 \text{ W/m}^2$ multiplied by three factors:

- 1) F_J accounts for the yearly *variation in the earth-sun distance*. The sun is nearest the earth around January 3rd. (This partly explains why winters in the Northern Hemisphere are somewhat milder than at corresponding latitudes in the Southern Hemisphere.) The following formula can be used to estimate F_J , where the "day number" can be found from an almanac or calendar.

$$F_J = 1 + 0.033 \cdot \cos \left(\frac{360 \cdot (\text{day} - 3)}{365} \right) \quad (2)$$

- 2) The factor a^L accounts for the *attenuation* (absorption plus scattering) of the direct solar irradiance during its passage through the atmosphere, where L is the air mass.
- 3) Finally the factor $\sin V$ takes the *geometry* of the situation into account for a solar elevation angle V . The solar elevation angle can be computed with knowledge of the latitude, the solar declination angle and the local time. The equation required is widely available in the solar energy design literature [1].

The air mass L through which the direct rays of the sun must pass depends of course on the solar elevation angle above the horizon. For angles $V > 25^\circ$ a simple drawing will reveal that the air mass $L = 1/\sin V$, for in this case it is reasonable to assume that the earth is a flat surface, and the atmosphere is a thin, flat layer above it. The curvature of the earth can be ignored. For example, if the angle $V = 30^\circ$, then $L = 1/\sin 30^\circ = 2$ air masses. However, for angles below 25° it becomes necessary to take the curvature of the earth and temperature gradients in the atmosphere into consideration, and the connection between the air mass and the solar elevation angle becomes more complex. Fritz Kasten and Andrew Young have developed a good, practical formula which is well suited for use with small solar elevation angles [2]:

$$L = \frac{1,002432 \sin^2 V + 0,148386 \sin V + 0,0096467}{\sin^3 V + 0,149864 \sin^2 V + 0,0102963 \sin V + 0,000303978} \quad (3)$$

Young's equation is not only valid for small angles; it works fine for angles up to and including 90° , for the above relationship asymptotically approaches $1/\sin V$ for angles above 25° . For example, if the angle $V = 90^\circ$ is entered into the above equation, one finds $L = 1,00$ as one should when the sun is at the zenith. Equation (3) has been used in the calculations of solar irradiance in this paper.

The term I_F in Equation (1) accounts for the diffuse irradiance on the horizontal surface due to scattering from the sky and from clouds. In previous work we have demonstrated how the diffuse irradiance depends upon atmospheric turbidity [3]. The *Linke turbidity factor* is a good measure of atmospheric clarity, being equal to unity for a "perfectly clear" Rayleigh atmosphere with no aerosol, about 3 for a typical day and around 8 for an exceptionally hazy atmosphere. The precise definitions can be viewed in the reference cited at www.soldata.dk under the heading "Download documents".

The model calculations (red graph) shown in Figure 3 are based on the radiation model just described. The model has been implemented in Excel. The input data required are:

- *latitude* and *longitude* of the location of interest and UTC
- the *day of the year* - this permits calculation of F_j using Equation (2)
- the *solar declination angle* permits computation of the solar elevation angle V
- the *air mass* L follows from Young's formula Equation (3) when V is known.

The only "adjustable" parameter in Equation (1) is the attenuation factor a . Fine tuning a in the Excel spreadsheet permits the radiation model to be fitted closely to the observed data. This fitting process can be carried out for entire blocks of data or for selected time intervals to reveal the best value of the atmospheric attenuation during the period of interest. To test the model we have applied it to data made available in a cooperative effort with Simme Eriksen in Uummannaq, Greenland. This calculation and the actual data are shown in Figure (4). The data from Greenland were collected using a SolData 80spc pyranometer.

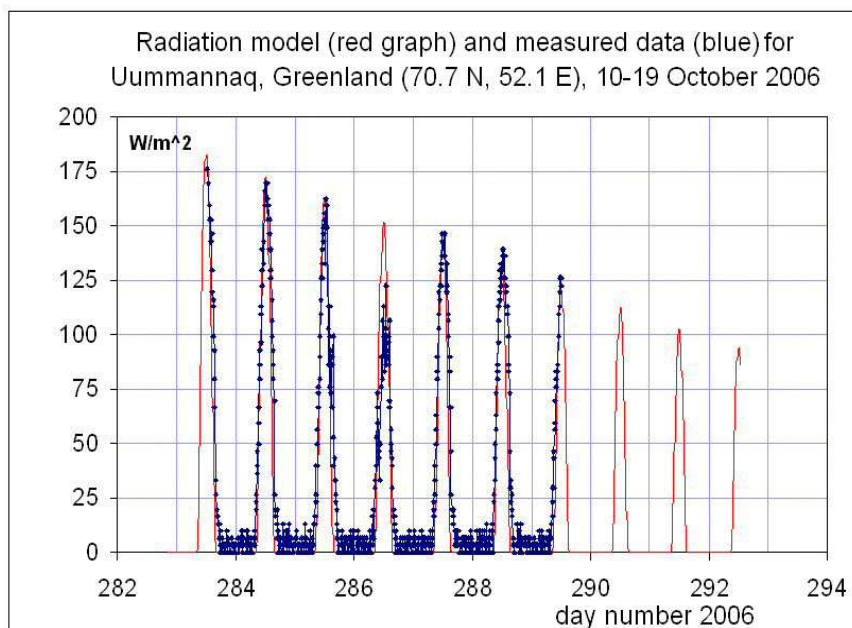


Figure 4: The data shown in this figure were collected by Simme Eriksen using a Sol-Data 80spc pyranometer. The red graph shows the model calculation for this very northern latitude. Typically for pristine Arctic locations, a value of the attenuation factor $a = 0.85$ yielded the best agreement with the data. Notice how the solar irradiance is decreasing day by day as the total darkness of the coming Arctic winter draws closer in late October.

The model yields best agreement with data in Arctic regions for values of a in the range from 0.8 to 0.9, while a value between 0.7 and 0.8 often yields best agreement in the tropics.

BAROMETRIC PRESSURE AND IONIZING RADIATION

The optics table included additional instrumentation as described previously. Due to restrictions of space in this paper, we will focus only on two quantities measured: the *barometric pressure* and the *radioactivity* measured by the GM counter. Although one would expect these parameters to be of only passing interest, we were in for a number of interesting surprises in the course of these observations:

- 1) The radioactive background radiation was nearly constant while the ship was at sea. In port or near coastlines significant increases in radioactivity often occurred.
- 2) There is an interesting correlation between the barometric pressure and the radioactive background radiation.
- 3) Global atmospheric pressure waves were observed. They were particularly noticeable at latitudes between the Tropic of Cancer and the Tropic of Capricorn.

Figure 5 shows one of the first surprises experienced with our moving data collection platform. When the ship laid to the quay near Amalienborg Castle in Copenhagen, the level of radioactivity increased by 50% compared with levels at sea. This was apparently due to the massive amounts of granite used to build the castle and surrounding facilities. Granite contains uranium-238 and its daughter isotopes (thorium, radium, radon, lead, polonium, etc.). Air-borne dust particles containing these isotopes cause the background radiation to rise. The same phenomenon can be observed at Grand Central Station in New York City where granite is the building material

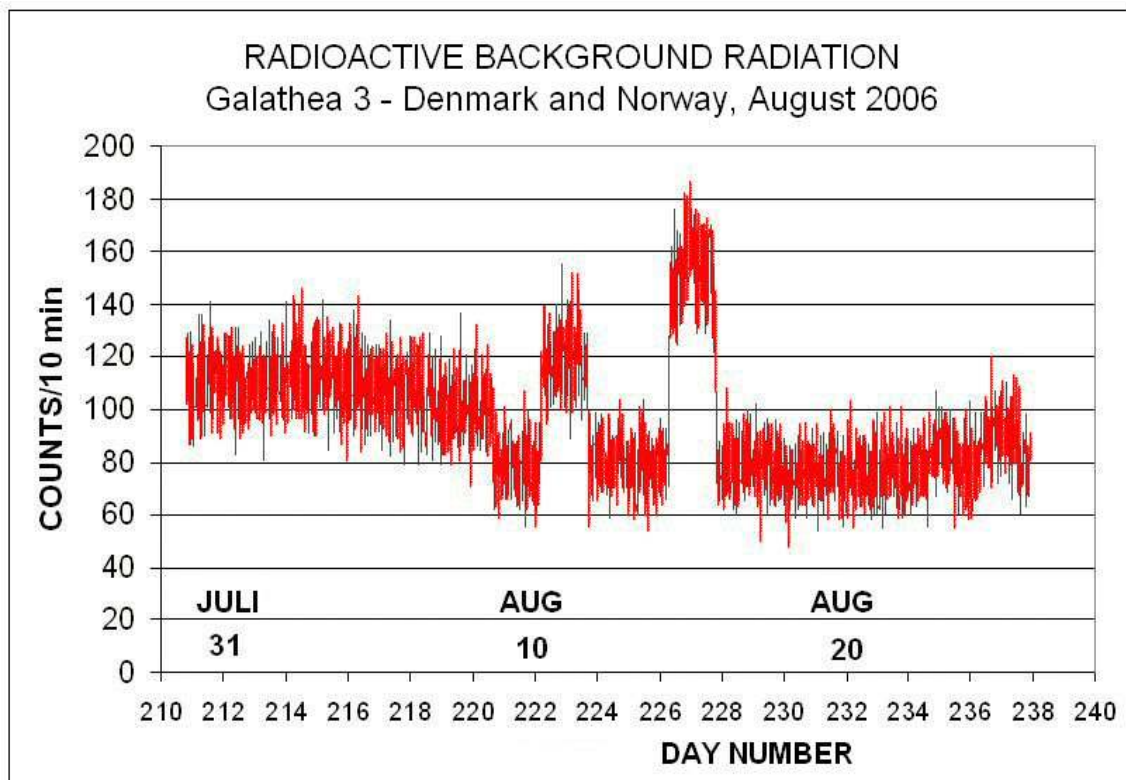


Figure 5: At sea the radioactive background radiation remained nearly constant around 80 counts every 10 minutes. Near coastlines or in port the background radiation would sometimes increase dramatically. The two peaks observed in this figure are from Amalie Quay in Copenhagen, Denmark, and from dry dock in Stavanger, Norway.

When the ship was pulled into dry dock in the Norwegian port city of Stavanger for maintenance, the background radiation level doubled, for the bedrock on all sides of the ship contained granite.

Figure 6 shows the correlation observed between the radioactive background radiation and the barometric pressure. When the atmospheric pressure is high, the attenuation of extraterrestrial radiation is slightly higher due to the greater airmass which must be penetrated by the radiation. The same phenomenon has been reported in the literature [4].

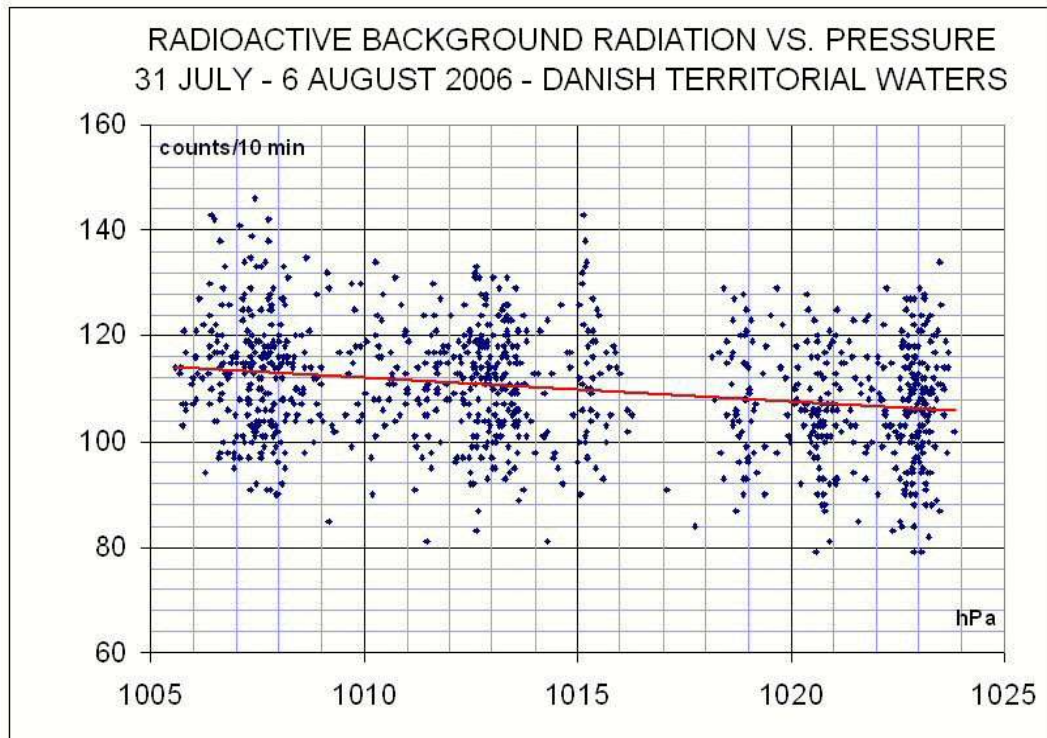


Figure 6: While in port these data were recorded showing the correlation between the radioactive background radiation and the atmospheric pressure.

Another surprise from our observations was the periodic oscillations in the atmospheric pressure with were particularly noticeable in the tropics. Figure 7 shows the variations observed near the equator on the coast of Africa near Accra, Ghana. Our first response was to look for an instrumentation error, air conditioning effects in the laboratory or to suspect the pressure changes due to land and sea breezes in coastal regions.

These hypotheses turned out to be wrong: e.g. the oscillations remained even in the middle of the Indian Ocean. Note that the period of the oscillations was close to 12 hours suggesting a solar rather than a lunar origin for the oscillations. (The period of lunar motion viewed from the earth is 12:25.) The pressure oscillations turned out to be due to *global atmospheric tides*. Their amplitude at the earth's surface is about 3-4 hPa and greater at higher altitudes.

The driving force is believed to be heating of the ozone layer by absorption of solar UV irradiance. An interaction of atmospheric tidal forces due to the sun and ozone layer heating is believed to be the cause of the observed oscillations. There is a substantial body of literature available on this interesting phenomenon [5].

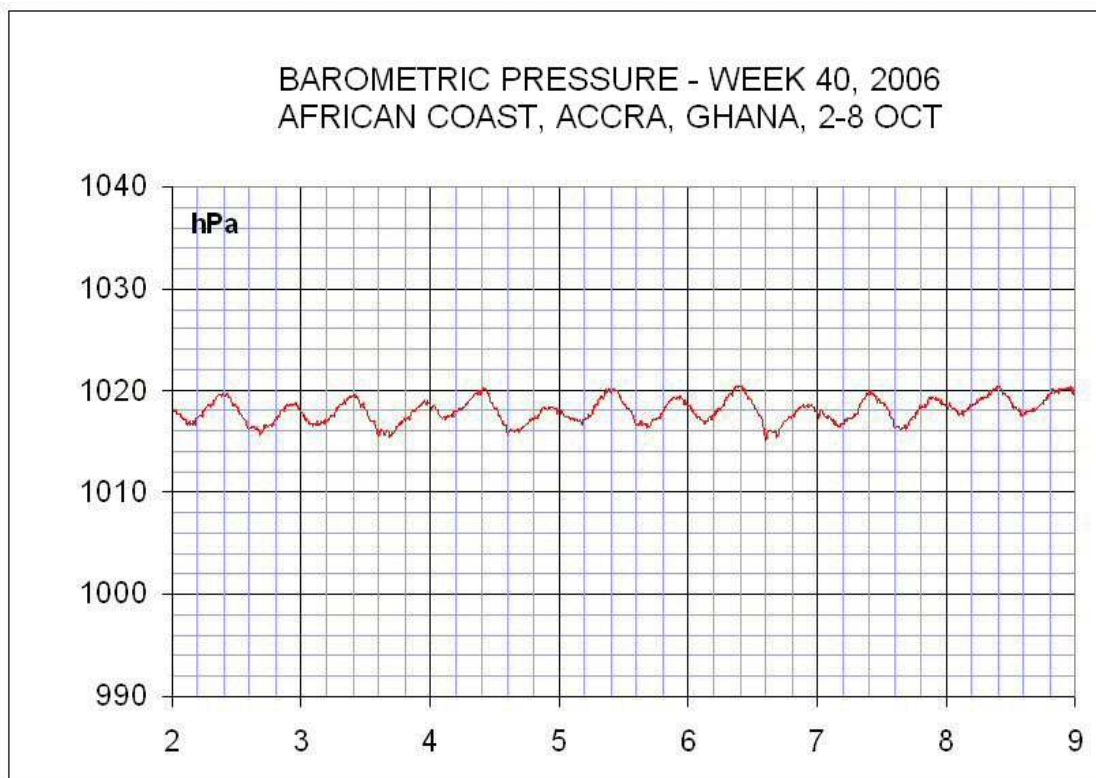


Figure 7: *When in the tropics systematic pressure variations with a period of close to 12 hours were observed. Note how every second wave top appears slightly smaller than the one before it.*

CONCLUSIONS

We have collected a large body of solar irradiance and other data during the eight month 100.000 kilometer voyage of the Danish research vessel *Vædderen* on the Galathea 3 Expedition. Our preliminary analysis has been described in this paper, and in the coming months a more complete analysis of the results will be carried out and reported at a subsequent ISES meeting. The data base and additional literature has been made accessible to all at www.soldata.dk.

REFERENCES

- [1] J.A. Duffie, W.A. Beckman; *Solar Engineering of Thermal Processes*, Wiley & Sons, New York, 1980, chapter 2.
- [2] F. Kasten, A.T. Young; *Revised optical air mass tables and approximation formula*, **Applied Optics**, **28**, no. 22, pp 4735-4738, 15 Nov 1989.
- [3] Frank Bason; *Diffuse Solar Irradiance and Atmospheric Turbidity*, **EuroSun 2004**, ISES Europe, June 2004, Proceedings.
- [4] T. Wibig, R. Pierzynski, R. Sobczak; *Educational studies of cosmic rays with a telescope of GM-counters*, **Physics Education**, Nov. 2006, pp 542-545.
- [5] For more about global atmospheric tides see e.g. www.answers.com/topic/atmospheric-tide or www.franksingleton.clara.net/atmospheric_tides.html